JCTC Journal of Chemical Theory and Computation

Article

pubs.acs.org/JCTC

Systematic Procedure To Parametrize Force Fields for Molecular Fluids

Frank José Salas,[†] G. Arlette Méndez-Maldonado,[†] Edgar Núñez-Rojas,[†] Gabriel Eloy Aguilar-Pineda,[‡] Hector Domínguez,[§] and José Alejandre*[,†]

[†]Departamento de Química, Universidad Autónoma Metropolitana-Iztapalapa, Av. San Rafael Atlixco 186, Col. Vicentina, 09340, México Distrito Federal, México

[‡]Colegio de Ciencia y Tecnología, Universidad Autónoma de la Ciudad de México, Fray Servando Teresa de Mier 99, 06080, México Distrito Federal, México

[§]Instituto de Investigaciones en Materiales, Universidad Nacional Autónoma de México, 04510, México Distrito Federal, México

Supporting Information

ABSTRACT: A new strategy to develop force fields for molecular fluids is presented. The intermolecular parameters are fitted to reproduce experimental values of target properties at ambient conditions and also the critical temperature. The partial charges are chosen to match the dielectric constant. The Lennard-Jones parameters, ε_{ii} and σ_{ii}, are fitted to reproduce the surface tension at the vapor−liquid interface and the liquid density, respectively. The choice of those properties allows obtaining systematically the final parameters using a small number of simulations. It is shown that the use of surface tension as a target property is better than the choice of heat of vaporization. The method is applied to molecules, from all atoms to a coarse-grained level, such as pyridine, dichloromethane, methanol, and 1-ethyl-3-methylimidazolium tetrafluoroborate (EMIM-BF4) at different temperatures and pressures. The heat of vaporization, radial distribution functions, and self-diffusion coeficient are also calculated.

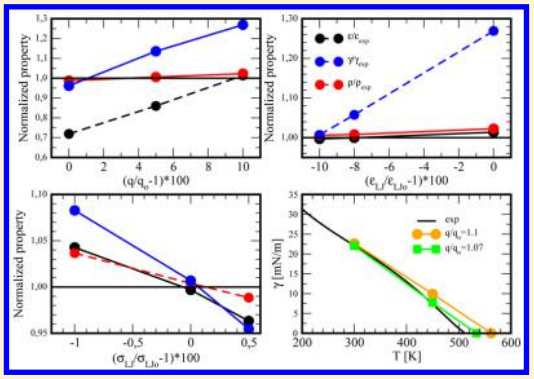

1. INTRODUCTION

Molecular simulation methods are powerful tools to determine macroscopic properties from microscopic interactions. The main ingredient to develop a simulation is the force field which determines the quality of predicted properties. During the last three decades a lot of efforts have been made to develop efficient and accurate force fields. When comparing simulation results with experimental data it is common to obtain the potential parameters to match some target experimental properties in the liquid phase. It is well accepted that the molecular geometry obtained from electronic structure calculations is in good agreement with experimental data. Thus, the intramolecular parameters are usually extracted from spectroscopic experiments or by quantum mechanical calculations of isolated molecules. The charge of an atom in a molecule is not well-defined, and its value depends strongly on the used level of theory. Force fields such as OPLS/AA,[1] GAFF,[2] and CHARMM[3] obtained the charges from highly accurate ab initio calculations. The partial charges sometimes have been scaled[4,5] to include, in an effective way, many body effects in a liquid, but it is not clear how the scaling factor has to be chosen. The Lennard-Jones, LJ, parameters can be fitted using molecular simulations to reproduce target experimental liquid properties such as density, ρ, radial distribution functions, and heat of vaporization, ΔH_{vap},[1,2,4,6,7] at ambient conditions. The force fields parameters obtained in that way, sometimes, are not able to reproduce the experimental critical temperature and orthobaric densities.[8]

Water is perhaps the more studied system by computer simulations. The TIP3P,[9] SPC/E,[10] and TIP4P[11] force fields were developed to reproduce the liquid density and heat of vaporization at ambient conditions, while the target properties for the TIP4P/2005[12] model were the temperature of maximum density and density of several ices. Vega et al.[13,14] in 2009 and 2011 evaluated rigid nonpolarizable models with three, four, and five sites and arrived to the conclusion that TIP4P/2005[12] was the best; however, that model predicted 58 for the dielectric constant, ε, at 298 K and 1 bar in comparison with the experimental value of 78.

Caleman et al.[15] in 2011 developed molecular dynamics simulations over 146 organic liquids to evaluate the efficiency of OPLS/AA and GAFF force fields in reproducing the experimental values of ρ, ΔH_{vap}, heat capacities, isothermal compressibility, volumetric expansion coefficient, dielectric constant, and surface tension, γ, at the liquid−vapor interface. In both force

Received: September 22, 2014
Published: December 18, 2014

DOI: 10.1021/ct500853q
J. Chem. Theory Comput. 2015, 11, 683−693

fields, the intramolecular parameters and charges were obtained from quantum mechanical calculations, while the LJ parameters were fitted to reproduce ρ and ΔH_{vap}. The main conclusions drawn by Caleman et al.[15] were that both force fields systematically predicted lower ε and γ with respect to experimental data. The dielectric constant is a measure of the dipole moment fluctuations; therefore, it is important to have force fields that reproduce the experimental value of that property to understand its role in solubility of systems containing charged atoms. It is well-known that, in simulations, the γ is strongly affected by truncation distance[16] of short ranged interactions and surface area.[17] Zubillaga et al.[18] found that the surface tensions reported by Caleman et al.[15] were not correct because their calculations were developed with a small truncation distance. The surface tension results reported by Zubillaga et al.[18] for the OPLS/AA force field agreed well with experiment; however, the increase of truncation distance left unchanged the dielectric constant. It has been argued that in order to reproduce the experimental dielectric constant it might be necessary to use polarizable force fields.[20] Including polarizability seems to be a good alternative to develop force fields because the electric field that surrounds a molecule is taken into account to modify the electrostatic interactions. Those models are computationally more expensive compared with those where the charges are fixed. Advances in that field have been made, but it is not possible to say that the issue is solved. Recently, the polarizable force field iAMOEBA[21] of water has been able to improve the results of the best nonpolarizable models. However, for other molecular systems the situation is not so good. More work is needed to find the best way to include polarizability at low computational cost.

Before starting to develop that kind of models it is convenient to explore with more detail the capabilities of nonpolarizable force fields to reproduce the dielectric constant.

Alejandre et al. developed in 2011 the nonpolarizable TIP4Q force field of water[22] using as target properties the dielectric constant and temperature of maximum density. It was shown in that work that the dielectric constant changes linearly with dipole moment and that it was almost independent to changes in the LJ parameters. Later on, in 2014, Fuentes and Alejandre[23] developed also the nonpolarizable TIP4P/ε model where a dipole moment of minimum density was found at 240 K that allowed fitting the geometry and charges in order to calculate the dielectric constant. Fuentes and Alejandre[23] found that changing the LJ parameters ε_{LJ}/k_B (where k_B is the Boltzmann constant) from 78 to 93 K and σ_{LJ} from 0.3154 to 3.165 nm modified the dielectric constant value in only three units. The procedure of finding the optimum molecular dipole moment was much faster in TIP4P/ε than in TIP4Q. The TIP4Q is 60% more computationally expensive than the TIP4P/ε, but both models gave excellent results compared with experimental data at different temperatures and pressures. Those works show that the long-range forces are almost independent from the LJ interactions when the dielectric constant is used as a target property.

Fennell et al.[24] in 2012 proposed a method to develop force fields of chloromethanes and SPC water using as target properties ρ, ε, and ΔH_{vap}. The charges were scaled to reproduce the dielectric constant. They observed that the effect of changing ε_{LJ} was more important on the ΔH_{vap} than in ε and ρ. The procedure proposed by Fennell et al.[24] to find the potential parameters to reproduce the experimental properties at room conditions consisted of changing linearly: first, all the σ_{LJ} values to reproduce ρ, second, all the charges to reproduce ε, and finally all ε_{LJ} to reproduce the ΔH_{vap}. The procedure was repeated up to four steps in order to obtain the optimum parameters. The new water model, $H_2O - DC$, developed by Fennell gave 255 K for the temperature of maximum density in contrast to the experimental value of 277 K. The model also fails to reproduce the experimental dielectric constant of water as a function of temperature.

In 2014, Wang et al.[25] developed the ForceBalance method to generate the parameters for the TIP3P-FB and TIP4P-FB force fields of water. The procedure involves highly detailed ab initio calculations over 100 000 cluster geometries extracted randomly from liquid−vapor and liquid−solid simulations for the polarizable iAMOEBA water model.[21] In addition, temperature and pressure dependence simulations were performed to obtain ρ, ΔH_{vap}, thermal expansion coefficient, isothermal compressibility, isobaric heat capacity, ε, and ice density. The final parameters of the TIP4P-FB force field were essentially the same as those reported by Fuentes and Alejandre for the TIP4P/ε model.

The heat of vaporization is directly related with the intermolecular potential energy of a liquid,[15] but it has to be corrected by adding an effective polarization[10,26] to compare with experimental data. That correction was added to increase the charges of the SPC force field to obtain the SPC/E model where the dielectric constant changed from 66 to 71. The polarization correction has not been used to develop most of the force fields that uses the ΔH_{vap} as a target property. On the other hand, the force fields based on ΔH_{vap} fail to reproduce the critical temperature. Siepmann and collaborators, to overcome that problem, developed the transferible potentials for phase equilibrium simulations, TraPPE,[27] where the potential parameters were adjusted to reproduce the critical temperature and saturated liquid densities. Parameters for that force field have been published for hydrocarbons,[27] methanol,[28] and amines,[29] among others. The parameters for hydrocarbons have also been obtained using the critical temperature and orthobaric densities using NERD force fields[30]

The use of dielectric constant as a target property in the fitting procedure does not improve the critical temperature. It is shown in this work that the force field developed by Fennell et al.[24] for dichloromethane to match ε has a critical temperature 100 K above the experimental value and overestimates the vapor pressure and γ at all temperatures.

The main goal of this work is to propose a systematic procedure to develop nonpolarizable force fields of molecular fluids taking advantage of the fact that electrostatic interactions are independent of the short ranged interactions if ε is used as a target property. It is shown that γ at the liquid−vapor interface can be used as a target property to fit the ε_{LJ} parameters. Until our knowledge, the surface tension has only been used as a target property to develop a coarse-grained force field of hydrocarbons.[31] The σ_{LJ} parameters in this work were fixed to match the experimental density. By performing an additional simulation at the liquid−vapor interface, a rough estimation of the critical temperature was obtained by assuming γ changes linearly with temperature.

The work is organized as follows: Section 2 describes the simulation details, the optimization procedure is explained in Section 3, the results and discussions are found in Section 4, and conclusions and references are given. Finally, the new force field parameters are given in the Appendix.

DOI: 10.1021/ct500853q
J. Chem. Theory Comput. 2015, 11, 683−693

2. SIMULATION DETAILS

Molecular dynamics in the liquid phase were performed in systems with 500 or 864 molecules using the isotropic isothermal−isobaric ensemble (NPT) to obtain ε and ρ. The surface tension was obtained in the canonical ensemble (NVT) using slab simulations with a liquid surrounded by a vapor for systems containing between 2000 and 3000 molecules. The simulations were carried out using the GROMACS 4.5.4 package,[32] and the equations of motion were solved using the leapfrog algorithm with a time step of 2 fs. The internal temperature was coupled to a Nosé−Hoover thermostat with a parameter τ_T = 0.5 ps, while the pressure was coupled to a Parrinello−Rahman barostat with a parameter τ_P = 1.0 ps. Orthogonal periodic boundary conditions were used in all directions. The bond distances were kept rigid by using the LINCS procedure. Except for pyridine and methanol where the bending angles were flexible, the dichloromethane and EMIM-BF4 were fully rigid, and the equilibrium geometry of those molecules is shown in Figure 1.

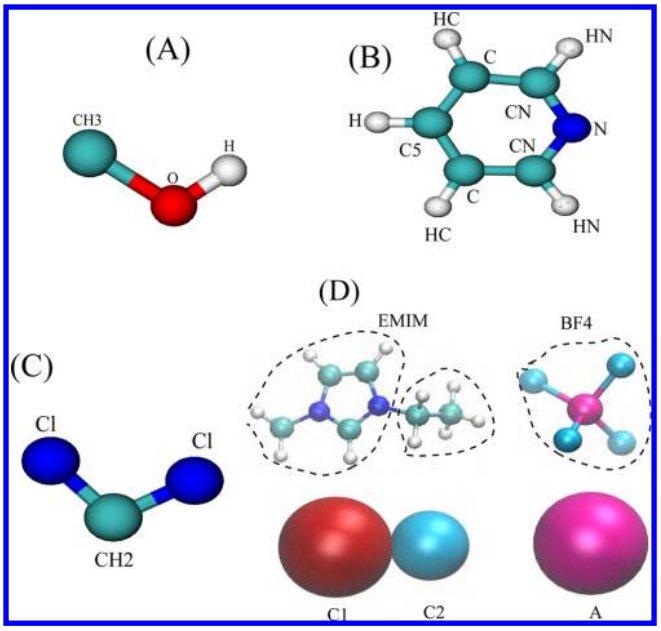

Figure 1. Molecular geometry of the systems studied in this work: A) methanol, B) pyridine, C) dichloromethane, and D) EMIM-BF4.

The electrostatic interactions were treated with the Ewald sum[33] with a tolerance of 1×10^{-6} for the real space contribution. The real part of the Ewald summation and the LJ interactions were truncated at 1.2 nm with added long-range corrections. The long-range contribution of electrostatic interactions was determined through the particle mesh Ewald method with a grid of reciprocal vectors of 1.2 nm and spline of order 4. The dielectric constant, obtained using the dipole moment fluctuations of the system, and density were calculated in the same simulation for at least 50 ns after an equilibration period of 10 ns. The surface tension, obtained using the average components of the pressure tensor, depends on truncation distance[16,18] and surface area;[17] therefore, the calculations were carried out using a truncation distance of 2.5 nm and dimensions of the simulation cell of at least $L_x = L_y$ = 5.0 nm; L_z was around $3L_x$. The equilibration period was 2 ns, and the average values were obtained for an additional 6 ns. The standard deviation was estimated from 3 blocks of 2 ns. The density profile was also obtained in the interface simulations, and the orthobaric densities were calculated from the average value in the bulk regions. The vapor pressure was obtained using the normal component of the pressure tensor.

3. OPTIMIZATION PROCEDURE

The procedure used in this work to obtain the optimum force field parameters involves the calculation of ε and γ. The dielectric constant requires long simulations to obtain reliable results, while the surface tension requires large system. The surface tension and vapor pressure were calculated using the mechanical definition of pressure for a planar interface. The calculation details can be found in the original sources.[16,18] For a planar interface, the mechanical stability requires that the gradient of the pressure tensor is zero everywhere in the fluid, and it implies that the normal pressure is a constant.[19] Nowaday, it is possible to develop in 1 day simulations for several ns of large systems due to the use of very fast parallel computers and efficient molecular simulation programs. The procedure proposed in this work is systematic, and it requires a small number of simulations to obtain the optimum parameters.

In this work, the procedure is focused on scaling linearly the intermolecular parameters to match four target experimental properties; however, the method is more general. The dielectric constant at the end is obtained using the molecular dipole moment. For a given new molecule, the geometry and charges can be obtained from electronic structure calculations. The dipole moment can be varied by scaling the charges or by changing the geometry. This is particularly important when the molecules are not planar and the torsional angles play an important role to define the composition of the system. By choosing the dielectric constant as a target property it is possible to find the optimum charges, geometry, and torsional barriers. It is a procedure to discard some results obtained by quantum mechanical calculations. The method also leads to optimum LJ parameters even if the original force field fails to reproduce the surface tension or density; that is the case of dichloromethane. The procedure followed in this work is as follows:

1) All charges are scaled to obtain ε.

2) With the new charges, all the ε_{LJ} values are scaled to determine γ.

3) With the new charges and new ε_{LJ}, all the σ_{LJ} values are scaled to obtain ρ.

4) With the optimum parameters the critical temperature is roughly estimated with additional simulations assuming a linear behavior of surface tension with temperature.

A reparameterization step can be performed if in the first cycle the relative error between simulation and experimental results of a given property is greater than the target tolerance.

4. RESULTS

In order to show the capabilities of the method, molecules with different levels of description are chosen: all-atoms (pyridine), united atoms (methanol and dichloromethane), and coarse-grained level (EMIM-BF4). In this work, the maximum relative error or target tolerance of a property X, defined as $\Delta X = |(X_{exp} - X_{MD})|*100/X_{exp}$, between the molecular dynamics and experimental was 8%, 5%, and 1% for ε, γ, and ρ, respectively, while the target tolerance for the critical temperature was 8%. For comparison, the average tolerances for ε, γ, and ρ of 146 liquids reported by Caleman et al.[15] for OPLS/AA were 43%,

DOI: 10.1021/ct500853q
J. Chem. Theory Comput. 2015, 11, 683−693

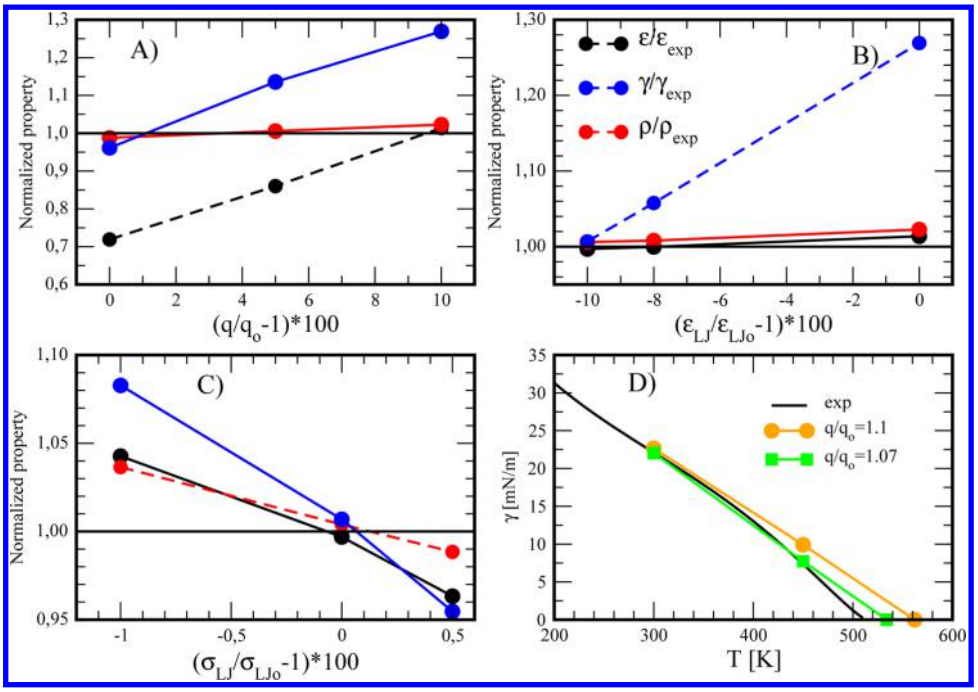

Figure 2. Systematic procedure to develop force field parameters of methanol: A) effect of changing charges, B) effect of changing ε_{LJ}, C) effect of changing σ_{LJ}, and D) rough estimation of the critical temperature using a linear correlation on the surface tension. The black continuous lines are results for the experimental values taken from dielectric constant,[38] surface tension,[39] and density.[40] The discontinuous lines are used for the target properties [dielectric constant in A), surface tension in B), and density in C)] for an easy identification. The dielectric constant and density were calculated at 298.15 K and 1 bar. The surface tension was obtained at 298.15 and 450 K.

22%, and 2%, respectively, and for GAFF 35%, 23%, and 4%, respectively. The initial parameters of every system, that can be taken from a known force field, are called in the rest of the manuscript "the original parameters" and they will be denoted with a subindex 0. To show the effect of changing the original parameters on the target properties it is convenient to express them as a ratio. For instance, the change of charges with respect to the original values is $(q/q_0 - 1) \times 100$. The equation gives a zero value for the original charges. The same definition is used for changes of ε_{LJ} and σ_{LJ}. The target properties, ε, γ, and ρ, were normalized by the corresponding experimental value; in that way, the relative error in every property is the difference between the calculated value and the experimental data, and it can be obtained directly from an inspection of a figure. The normalized experimental value of all the target properties is always one as it is shown in Figure 2. All the numerical data for all the systems are given as Supporting Information. The results from this work with the new parameters are shown with the legend MD.

4.1. Methanol. The initial force field parameters, fitted to reproduce the liquid−vapor coexisting densities as a function of temperature and the critical temperature, were taken from the TraPPE force field.[28] The cross interactions for the LJ parameters were calculated using the Lorentz−Berthelot mixing rules. The molecule is rigid in bond distances and flexible in the bending angle, and the methyl group is treated as a united atom. The intramolecular parameters were as follows: r_0(CH3−O) = 0.143 nm, r_0(O−H) = 0.0945 nm, θ_0(CH3−O−H) = 108.5, and k_θ = 460.67 kJ/(mol rad^{-2}). The calculated values of ρ and γ with the original parameters, a value of zero in the X axis of Figure 2-A, are in excellent agreement with experimental data. The TraPPE force field, at room conditions, predicts a dielectric constant of 23 and that value was calculated in this work. It is 28% smaller than the experimental value of 32, see Figure 2-A.

The results of target properties when all the charges are scaled keeping constant the rest of the original parameters are shown also in Figure 2-A. The charges were increased by 10% to reproduce the dielectric constant. The surface tension and density increased by 32% and 3%, respectively. The value of zero in the X axis in Figure 2-B is for results obtained with the new charges and the rest of original parameters constant, including ε_{LJ}. The original ε_{LJ} parameters were decreased by 10% to reproduce the surface tension, which decreased 26%, as shown in Figure 2-B. The dielectric constant and density decreased only 2.5%. The value of zero in the X axis in Figure 2-C is for results obtained with the new charges and new ε_{LJ} leaving constant the rest of the original parameters, including σ_{LJ}. The results obtained with the new σ_{LJ} are shown in Figure 2-C. The properties change linearly with changes in σ_{LJ}; however, it is seen that all the properties with zero in the X axes are within the required tolerance, and therefore a change on σ_{LJ} values was not performed.

Every target property changed linearly, within simulation error, with its correponding changes on the force field parameters; therefore, the optimum values of every parameter might be estimated by performing three simulations, two to find a linear equation and a third to match the experimental data.

The final step of the fitting procedure was to evaluate the capabilities of the optimum parameters, obtained at ambient conditions, to predict the properties as a function of temperature. The procedure is shown for methanol in Figure 2-D. The surface tension at the critical point is zero; therefore assuming that it changes linearly with temperature, it is possible to have a rough estimation of the critical temperature by performing an additional simulation close to that temperature, at 450 K in this case. With the surface tension results from simulations with the

DOI: 10.1021/ct500853q
J. Chem. Theory Comput. 2015, 11, 683−693

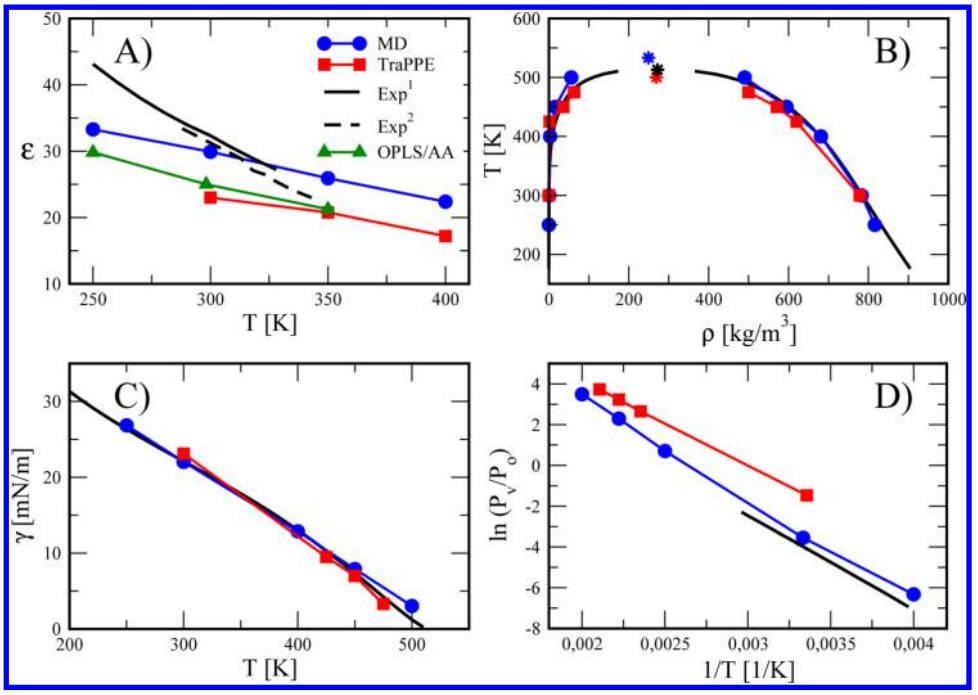

Figure 3. Thermodynamic properties of methanol as a function of temperature. The results for the TraPPE model were obtained in this work. A) Dielectric constant and the experimental values are shown with continuous[38] and discontinuous[41] lines. B) Coexisting densities and the experimental data are those reported by Smith and Srivastava.[40] C) Surface tension and the experimental data are from ref 39. C) Vapor pressure and the experimental data are from ref 40. The experimental critical temperature was taken from ref 28.

new parameters, a linear equation was fitted, and the critical temperature was obtained by extrapolation. The linear assumption on surface tension allows a rapid evaluation of the final parameters to reproduce the effect of temperature also in density. Of course, the correct value of the critical temperature has to be obtained with more simulations close to the critical point. The results for methanol are shown in Figure 2-D where it is seen that when the original charges were increased by 10% the extrapolated critical temperature was 562 K with a relative error of 8.4%, higher than the required tolerance of 8%. The slope of the line can be modified by changing the charges. The estimated critical temperature was obtained within the tolerance when the original charges were scaled by 7% and the dielectric contant at 300 K was 30; both values lie within the tolerance. The surface tension and liquid density at 300 K using the new charges were within the tolerance, and therefore it was not necessary to reparameterize ε_{LJ} and σ_{LJ}. The final force field parameters for methanol are given in the Appendix.

Figure 3 shows the results of methanol for dielectric constant, orthobaric densities, surface tension, and vapor pressure as a function of temperature. The results for the TraPPE force field with the original parameters were obtained in this work to make a comparison using the same conditions in the simulations. The new results were in excellent agreement with those reported in the original sources.[28] Figure 3 shows only the new results. The new force field improves the dielectric constant betwen 250 and 350 K, but TraPPE seems to be better after 350 K, see Figure 3-A. The dielectric constant of methanol as a function of temperature was calculated using the OPLS/AA model in order to analyze if the difference between the calculated values and experimental results was due to the united atom approximation used for CH_3. The results shown in Figure 3 were similar to TraPPE and shifted to lower values with respect to the new model. The united atom approximation does not improve the results of the dielectric constant. The liquid−vapor phase diagram is shown in Figure 3-B. The new parameters improve the TraPPE liquid densities close to the critical point. The critical temperature obtained using the rectilinear diameters law with critical exponent 0.32 was 533 K, slightly different than that obtained by extrapolation using the surface tension during the fitting procedure. The critical temperature obtained in this work using the TraPPE parameters was 500 K, while the reported value by Chen[28] was 502 K. The experimental data is 513 K. The surface tension is shown in Figure 3-C; there is an excellent agreement between results from both models and with experimental data. Figure 3-D shows the vapor pressure in a Claussius-Clapeyron version. The new parameters are in excellent agreement with experiment, and they improve the results from the TraPPE model.

The heat of vaporization was obtained in two ways: first using the difference between the vapor and liquid enthalpies, $\Delta H_v = H_{gas} - H_{liq}$, and second, through the slope of a Claussius-Clapeyron linear equation for the vapor pressure as a function of inverse temperature. The value of H_{gas} was estimated by developing a calculation of an isolated molecule. The results for TraPPE using both procedures were 38.8 and 34.5 kJ/mol, respectively. The model with the new parameters gave 47.3 and 41.1 kJ/mol. The experimental value at 300 K is 39.5 kJ/mol. The pair−pair radial distribution functions were almost unaffected by the use of the new parameters. The self-diffusion coefficient was 0.9×10^{-9} m^2/s which was compared with the values of 2.4×10^{-9} m^2/s and 2.2×10^{-9} m^2/s for the experimental value and the TraPPE model. The results of methanol are given as Supporting Information.

4.2. Pyridine. The procedure to search the parameters for pyridine is shown in Figure 4. The original intra- and intermolecular parameters of the OPLS/AA force field were taken from the Web page http://www.virtualchemistry.org. The parameters

DOI: 10.1021/ct500853q
J. Chem. Theory Comput. 2015, 11, 683−693

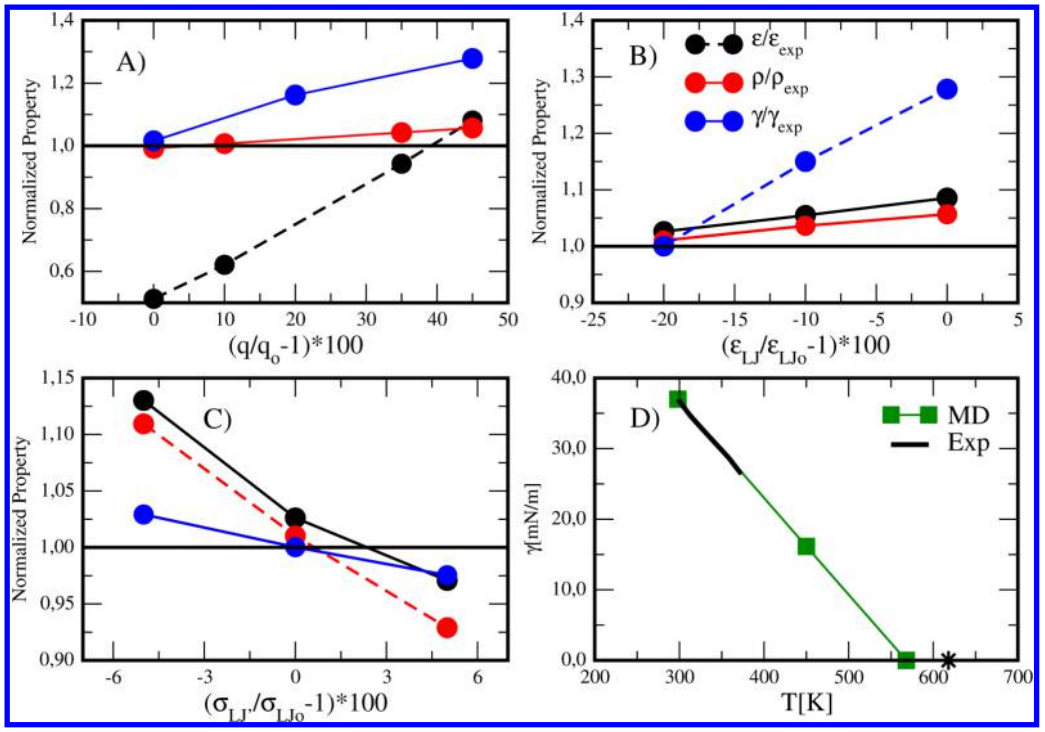

Figure 4. Systematic procedure to develop force field parameters of pyridine: A) effect of changing charges, B) effect of changing ε_{LJ}, C) effect of changing σ_{LJ}, and D) rough estimation of the critical temperature using a linear correlation on the surface tension. The continuous lines are results for the experimental values taken from dielectric constant,[39] surface tension, and density.[42] The discontinuous lines are used for the target properties [dielectric constant in A), surface tension in B), and density in C)] for an easy identification. The dielectric constant and density were calculated at 298.15 K and 1 bar. The surface tension was obtained at 300 and 450 K.

for intramolecular interactions were as follows: r_0 = 0.108 nm for bonds (CN−HN, C−HC, C5−H, CN−HN), r_0 = 0.140 nm for (CN−C, C−C5, C−CN), and r_0 = 0.1339 nm for (CN−N). The bending angles parameters were as follows: (θ_0, k_θ) = (120, 292.88 kJ/mol rad^2) for angles (HN−CN−C, CN−C−HC, HC−C−C5, C−C5−H), (120, 585.76 kJ/mol rad^2) for angles (C−CN−N), (166, 292.88 kJ/mol rad^2) for angles (HN−CN−N), (124, 585.76 kJ/mol rad^2) for angles (C−CN−N), and (117, 585.76 kJ/mol rad^2) for angles (CN−N−CN). The dihedral angles were given by the Ryckaert and Bellemans potential; the parameters were the same for all the angles: [c_0 = 30.334, c_1 = 0.0, c_2 = −30.334, c_3 = c_4 = c_5 = 0.0] kJ/mol. The cross interactions were calculated using the geometric mixing rules for the LJ parameters. The calculated values of density and surface tension with the original parameters, a value of zero in the X axis of Figure 4-A, are in excellent agreement with experimental data; however, the dielectric constant is almost half. In the first step of the fitting procedure, the original charges were scaled linearly more than 40% to reach the experimental dielectric constant; that change in charge increased the surface tension and density to around 30% and 5%, respectively. The value of zero in the X axis in Figure 4-B is for results obtained with the new charges and the rest of the original parameters constant, including ε_{LJ}. The initial values of the normalized target properties were the final values shown in Figure 4-A. In the second step of the fitting procedure, all the original ε_{LJ} values were scaled linearly keeping constant the charges obtained in the first step and the rest of the original parameters. After decreasing ε_{LJ} by around 20% the surface tension reached the experimental value, and the change in dielectric constant and density was around 5%. Decreasing ε_{LJ} by 20% returned the density close to its experimental value. The value of zero in the X axis in Figure 4-C is for results obtained with the new charges and the new ε_{LJ} leaving constant the rest of the original parameters, including σ_{LJ}. The results obtained with the new σ_{LJ} are shown in Figure 4-C. The density changes linearly with changes in σ_{LJ}. It is seen from the figure that the comparison with experiment can be improved if σ_{LJ} is increased by around 1%; however, the values of all the properties with coordinate X = 0 are within the required tolerance, and therefore a change on σ_{LJ} values was not performed.

The last step of the fitting procedure is to evaluate the new parameters to reproduce the critical temperature. A simulation at 450 K was performed to obtain the surface tension at the liquid−vapor interface, see Figure 4-D. The relative error of the critical temperature with respect to the experimental value was 8.1%, around the target tolerance of 8%. Therefore, a reparameterization of the force fields parameters was not perfomed. The number of simulations to obtain the optimum parameters for pyridine was less than in methanol. The final parameters are given in the Appendix.

The results of pyridine for dielectric constant, liquid−vapor phase coexistence, surface tension, and vapor pressure are shown in Figure 5. The dielectric constants at all temperatures for the new parameters are in excellent agreement with experiment; however, as expected, the property is underestimated by the OPLS/AA force field, see Figure 5-A. The orthobaric densities for the OPLS/AA and new force fields parameters are in excellent agreement. The critical temperature predicted by the new model using the reactilinear diameters law with a critical exponent of 0.32 was 590 K ± 3, see Figure 5-B, and the relative error with experimental data is lower than the target tolerance. Figures 5-C and 5-D show the surface tension and vapor pressure as a function of temperature. The results from

DOI: 10.1021/ct500853q
J. Chem. Theory Comput. 2015, 11, 683−693

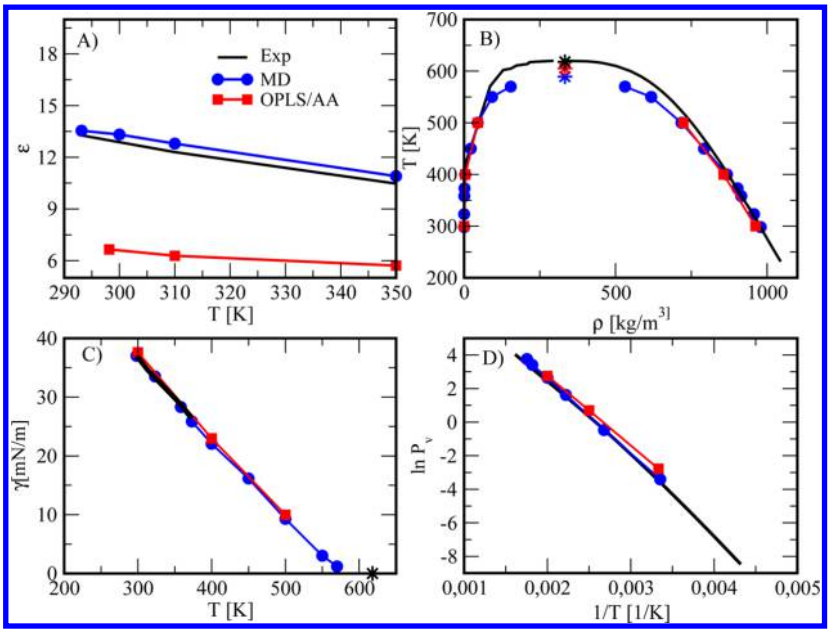

Figure 5. Thermodynamic properties of pyridine as a function of temperature. The results for the OPLS/AA model were obtained in this work. The legend MD is for results with the new set of parameters. The continuous lines are for experimental data. A) Dielectric constant and the experimental values were taken from ref 39. B) Orthobaric densities and the experimental data are from ref 42. C) The surface tension and the experimental values were taken from ref 42. D) Vapor pressure and the experimental data are from ref 43.

both models are in excellent agreement with experimental data. The critical temperature estimated for OPLS/AA was 605 K.

The results of ΔH_v for OPLS/AA using both procedures explained for methanol were 39.1 and 34.5 kJ/mol, respectively. The model with the new parameters gave 43.1 and 37.2 kJ/mol. The experimental value at 300 K is 40.1 kJ/mol. The pair−pair radial distribution functions were almost unaffected by the use of the parameters. The self-diffusion coefficient for pyridine at 300 K and 1 bar with the new set of parameters was 1.0×10^{-9} m^2/s, while that for the OPLS/AA model was 1.2×10^{-9} m^2/s. The experimental value is 1.5×10^{-9} m^2/s. The results of pyridine are given as Supporting Information.

4.3. Dichloromethane. The original parameters for dichloromethane were taken from the work of Fennell et al.,[24] and they were fitted to reproduce, at ambient conditions, ε, ρ, and ΔH_{vap}. The molecules were fully rigid. The cross interactions were calculated using the Lorentz−Berthelot mixing rules for the LJ parameters. The intramolecular parameters were as follows: r_0(CH2−Cl) = 0.18215 nm and r_0(Cl−Cl) = 0.29334 nm. The procedure used by Fennell et al. to parametrize dichloromethane will be compared with the one proposed in this work. Therefore, molecular dynamics simulations of liquids at 300 K and 1 bar were performed using the original parameters to check if our calculations agreed with those reported by Fennell et al. and also to avoid differences due to different simulation conditions. The comparison of results for different properties is given as property = (Fennell, this work): molecular dipole moment = (2.1, 2.1) D, dielectric constant = (8.8, 8.9), density = (1316.3, 1317.0) kg/m^{-3}, ΔH_{vap} = (28.74, 36.2) kJ/mol, self-diffusion coefficient = (2.13, 2.3) 10^{-9} m^2/s. The ΔH_{vap} obtained in this work, without adding any correction, was $-\langle U_{inter}\rangle/N+RT$, where $\langle U_{inter}\rangle$ is the average intermolecular energy of N molecules, R is the ideal gas constant, and T is the temperature. Fennell et al. used the same definition. The liquid density was also calculated as a function of temperature and 1 bar; the results from this work with the original parameters, filled squares in Figure 6, were the same as those

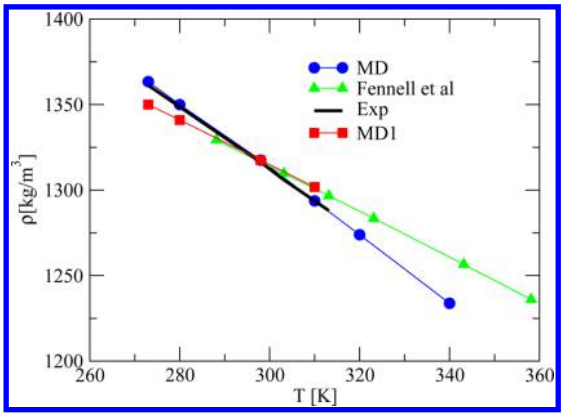

Figure 6. Liquid density of dichloromethane at different temperatures and 1 bar. The legends MD and MD1 are results from this work using the new set of parameters and those reported by Fennell et al.,[24] respectively. The results reported by Fennell et al. are shown with filled triangles. The experimental data were taken from ref 44.

reported by Fennell et al., but they were different from the experimental data. The results from this work for all the properties, using the original parameters reported by Fennell et al., agreed well with those reported for them except ΔH_{vap}; therefore, we are confident that our calculations were correct. With the new set of parameters, see filled circles in Figure 6, the density is in excellent agreement with experimental data at all temperatures. The surface tension was not reported by Fennell et al., and then a molecular dynamics at 300 K was performed in this work to evaluate the ability of the original parameters to predict that property. The result was 43 mN/m in contrast to the experimental value of 27 mN/m. The critical temperature was estimated using two values of surface tension, and the calculated value was 100 K higher than the experimental data. It is seen that the model proposed by Fennell et al. fails to reproduce also the surface tension at 300 K and the critical temperature.

DOI: 10.1021/ct500853q
J. Chem. Theory Comput. 2015, 11, 683−693

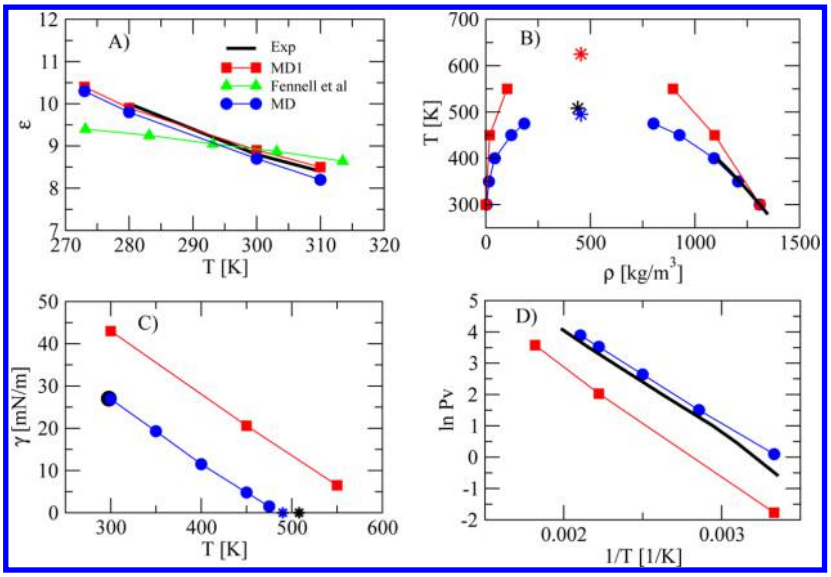

Figure 7. Thermodynamic properties of dichloromethane as a function of temperature. A) Dielectric constant, the legends MD and MD1 are results from this work using the new set of parameters and those reported by Fennell et al.,[24] respectively. The results reported by Fennell et al.[24] are shown with filled triangles. The experimental data were from ref 39. B) Orthobaric densities and the experimental values for liquid density were from ref 44, and the critical temperature is from ref 45. C) Surface tension and the experimental values were from ref 46. D) Vapor pressure and the experimental values were from ref 45.

The original charges reported by Fennell et al.[24] were unchanged in the first step of the fitting procedure because the reported dielectric constant at 300 K was already in good agreement with experiment. We also repeated the calculations at different temperatures to obtain the dielectric constant using the original parameters. The dielectric constant results are shown with filled triangles in Figure 7-A; they were different from those reported by Fennell shown with filled squares. The results with the new parameters are in excellent agreement with experiment at all temperatures.

The original ε_{LJ} parameters were decreased by 20% to match the experimental surface tension, but the liquid density decreased by 6.5%, and then the original σ_{LJ} values were increased by 3.1% to have the target properties within the required tolerance. The target properties obtained after applying the fitting procedure were within the requested tolerance. The charges were the same as the original values. The rough estimation of the critical temperature using the new parameters to determine the surface tension at 300 and 450 K was around 5% of the experimental value, and then a reparameterization was not necessary. The number of simulations to obtain the optimum parameters was less than in methanol. The final parameters are given in the Appendix.

The results of dichloromethane as a function of temperature are shown in Figure 7. The calculated dielectric constant using the new set of parameters is in excellent agreement with the results obtained using the force field parameters reported by Fennell et al.,[24] see Figure 7-A; the agreement with experiment is also excellent. We evaluated the ability of the new parameters to describe the coexisting densities and surface tension as a function of temperature. The results from this work show that the Fennell force field overestimates the orthobaric densities, surface tension, and vapor pressure at all temperatures, see Figure 7-B, Figure 7-C, and Figure 7-D, respectively. The critical temperature estimated from simulations using the new parameters is within the target tolerance. The vapor pressure with the new parameters is in excellent agreement with experiment at all temperatures.

The heat of vaporization at 300 K was calculated through the slope of a Claussius-Clapeyron linear equation for the vapor pressure. The experimental data is 27.6 kJ/mol. The result for the new model at 300 K was 25.8 kJ/mol, while that obtained in this work for the original model was 29.2 kJ/mol, compared with 36.2 kJ/mol obtained using the intermolecular energy. The self-diffusion coefficient at 298 K and 1 bar for the model with the new parameters is 3.0×10^{-9} m^2/s in comparison with the experimental value of 3.3×10^{-9} m^2/s.

4.4. EMIM-BF4. The optimization procedure was also applied to an ionic liquid at room temperature, EMIM-BF4, at a coarse-grained level. The EMIM ion was a rigid dimer with one site carrying a positive charge. The BF4 is modeled by one charged site to warrant electroneutrality in the system. The EMIM model used by Merlet et al.[34] contained three charged sites and required three charges and eight LJ parameters. The model proposed in this work has one charge and four LJ parameters. The cross interactions for the LJ parameters were calculated using the Lorentz−Berthelot mixing rules. The charge for BF4 in this work was taken from Merlet et al.,[34] and the same value was assigned to the charged site on EMIM. The starting point to simulate the EMIM-BF4 was to use sites with the same values of σ_{LJ} = 0.492 nm and ε_{LJ} = 1.9 kJ/mol and a bond length of 0.32 nm. The ε_{LJ} and σ_{LJ} of the uncharged site were fitted to reproduce at 400 K, within the target tolerance, the surface tension, and liquid density. The ionic liquids are, in general, not stable at high temperatures; they form other products, and therefore it is not possible to measure their critical temperature. The final parameters are given in the Appendix.

The results as a function of temperature are shown in Figure 8-A for density and in Figure 8-B for surface tension at the liquid−vapor interface. There are three sets of experimental data for densities that have slightly different values.[35−37] The results published by Shamsipur et al.[35] were used in this work

DOI: 10.1021/ct500853q
J. Chem. Theory Comput. 2015, 11, 683−693

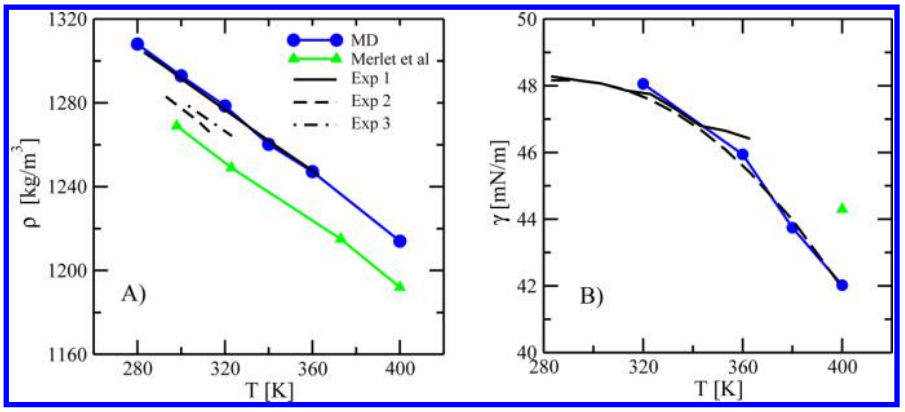

Figure 8. Thermodynamic properties of EMIM-BF4 at different temperatures at a coarse-grained level. A) Liquid density and the experimental data are shown with continuous,[35] dashed,[36] and dotted-dashed[37] lines, whereas the Merlet et al. simulation results are shown with filled triangles. B) Surface tension and the experimental data are from ref 35. The experimental values were fitted to a polynomial function of second degree[35] as shown with a black dashed line.

to parametrize the EMIM-BF4. The densities obtained with the new parameters are in excellent agreement with experimental data at all temperatures, while the results reported by Merlet et al. are systematically lower. The difference might be due to the use of different experimental data to fit the force field parameters. The surface tension for EMIM-BF4 systems as a function of temperature follows a linear equation at high temperatures, as it is found in many fluids, but it is a quadratic function when the whole range of temperatures is taken into account. The surface tension at 400 K reported by Merlet et al. was 44.3 mN/m in comparison with the experimental value of 41.9 mN/m, the relative error is 5.7%, and it is slightly larger than the target tolerance. The surface tension obtained at the same temperature with the new model is 42 mN/m.

5. CONCLUSIONS

The procedure proposed in this work to obtain force field parameters of molecular fluids is systematic and requires a small number of simulations. The charges or more general, the molecular dipole moment, can be fitted using the dielectric constant as a target property. The charges obtained from high accurate ab initio calculations can be used as starting values in the parametrization procedure, but after the scaling, they are empirical. The change of the dipole moment can be seen as an addition of an effective polarization to take into account the electric field of the surrounded medium around a molecule.

The choice of surface tension as a target property allows finding the optimum ε_{LJ} parameters leaving almost unchanged the dielectric constant. It is interesting to observe that the change in density due to the increase of charges is canceled with the decrease of ε_{LJ}; therefore, in methanol and pyridine the original parameters of σ_{LJ} were unchanged. In the case of dichloromethane the original σ_{LJ} values were increased to compensate the effect that ε_{LJ} had on the density. The results of the dielectric constant obtained in this work using the original and the new parameters for dichloromethane are the same, within the simulation error; that means the effect of LJ parameters on that property is small or negligible. The rough estimation of the critical temperature, within a tolerance, is performed efficiently using two values of surface tension, and it helps to obtain the optimum parameters valid for different temperatures and pressures with a small number of simulations.

The surface tension is a well-defined macroscopic property, and it is well-known how to calculate it in molecular simulations, and the comparison with experiment is direct. In contrast, some corrections, which in general are not easy to estimate, are needed to compare the calculated ΔH_{vap} with experimental data. The method proposed in this work, using the surface tension as a target property to obtain ε_{LJ}, improves not only the method that uses ΔH_{vap} but also that which is based on saturated densities and critical temperature as is the case of TraPPE. The optimum parameters for the ionic liquid, using a coarse-grained level of description, are able to reproduce the surface tension and density as a function of temperature.

The self-diffusion coefficient calculated using the new set of parameters are systematically lower compared with experimental data. If the target tolerances in dielectric constant, surface tension, and liquid density are slightly increased, then it might be possible also to include the experimental self-diffusion coefficient in the process of parametrization. Work in that direction is being performed.

Table 1

site	q [e]	ε_{LJ} [kJ/mol]	σ_{LJ} [nm]
Methanol			
CH3	0.284	0.7334	0.375
O	−0.749	0.6960	0.302
H	0.465	0.000	0.000
Pyridine			
CN	0.686	0.234	0.355
HN	0.017	0.100	0.242
C	−0.648	0.234	0.355
HC	0.225	0.100	0.242
C5	0.329	0.234	0.355
H	0.094	0.100	0.242
N	−0.983	0.569	0.325
Dichloromethane			
CH2	0.40440	1.0255	0.3603
Cl	−0.20220	1.0255	0.3421
EMIM-BF4			
A	−0.780	1.900	0.492
C1	0.780	1.900	0.492
C2	0.000	1.000	0.344

APPENDIX

Charges and LJ parameters for the systems studied in this work are obtained using the procedure described in Section 3. The

DOI: 10.1021/ct500853q
J. Chem. Theory Comput. 2015, 11, 683−693

sites names correspond to those shown in Figure 1. The force field parameters are given in Table 1.

■ ASSOCIATED CONTENT

Supporting Information

The numerical results of thermodynamic properties and selected pair distributions for the systems studied in this work. This material is available free of charge via the Internet at http://pubs.acs.org.

■ AUTHOR INFORMATION

Corresponding Author

*E-mail: jra@xanum.uam.mx.

Notes

The authors declare no competing financial interest.

■ ACKNOWLEDGMENTS

The authors would like to thank Humberto Saint-Martin for helpful comments and discussions. The allocation of computer time is acknowledged to Laboratorio de Supercómputo. GEAP thanks J. Alejandre at UAM-Iztapalapa for his hospitality during his sabatical year. F.J.S. and E.N.R. thank Conacyt for a graduate and posdoc scholarships, respectively. J.A. thanks Conacyt for financial support, project SEP-Conacyt 105843.

■ REFERENCES

(1) Jorgensen, W. L.; Maxwell, D. S.; Tirado-Rives, J. Development and all-atom Force Field on Conformational Energetics and Properties of Organic Liquid. *J. Am. Chem. Soc.* **1996**, *118*, 11225−11236.

(2) Wang, J.; Wolf, R. M.; Caldwell, J. W.; Kollman, P. A.; Case, D. A. Development and Testing of a General Amber Force Field. *J. Comput. Chem.* **2004**, *25*, 1157−1174.

(3) Bernard, R. B.; Robert, E. B.; Barry, D. O.; David, J. S.; Swaminathan, S.; Karplus, M. CHARMM: A Program for Macromolecular Energy, Minimization, and Dynamics Calculations. *J. Comput. Chem.* **1983**, *4*, 187−217.

(4) Jorgensen, W. L.; Swenson, C. J. Optimized Intermolecular Potential Functions for Amides and Peptides. Structure and Properties of Liquid Amides. *J. Am. Chem. Soc.* **1985**, *107*, 569−578.

(5) Jorgensen, W. L. Optimized Intermolecular Potential Functions for Liquid Alcohols. *J. Phys. Chem.* **1986**, *90*, 1276−1284.

(6) McDonald, N. A.; Jorgensen, W. L. Development of an All-Atom Force Field for Heterocycles. Properties of Liquid Pyrrole, Furan, Diazoles, and Oxazoles. *J. Phys. Chem. B* **1998**, *102*, 8049−8059.

(7) Jorgensen, W. L.; McDonald, N. A. Development of an all-atom force field for heterocycles. Properties of liquid pyridine and diazenes. *J. Mol. Struct.: THEOCHEM* **1998**, *424*, 145−155.

(8) van Leeuwen, M. E.; Smit, B. J. Molecular Simulation of the Vapor-Liquid Coexistence Curve of Methanol. *J. Phys. Chem.* **1995**, *99*, 1831−1833.

(9) Jorgensen, W. L.; Chandrasekhar, J.; Madura, J. D.; Impey, R. W.; Klein, M. L. Comparison of Simple Potential Functions for Simulating Liquid Water. *J. Chem. Phys.* **1983**, *79*, 926−935.

(10) Berendsen, H. J. C.; Grigera, J. R.; Straatsma, T. P. The Missing Term in Effective Pair Potentials. *J. Phys. Chem.* **1987**, *91*, 6269−6271.

(11) Jorgensen, W. L.; Chandrasekhar, J.; Madura, J. D.; Impey, R. W.; Klein, M. L. Comparison of Simple Potential Functions for Simulating Liquid Water. *J. Chem. Phys.* **1983**, *79*, 926−935.

(12) Abascal, J. L. F.; Vega, C. A General Purpose Model for the Condensed Phases of Water: TIP4P/2005. *J. Chem. Phys.* **2005**, *123*, 234505−234517.

(13) Vega, C.; Abascal, J. L. F.; Conde, M. M.; Aragones, J. L. What Ice can teach us about Water Interactions: A Critical Comparison of the Performance of Different Water Models. *Faraday. Discuss.* **2009**, *141*, 251−276.

(14) Vega, C.; Abascal, J. L. F. Simulating Water with Rigid Non-Polarizable Models: A General Perspective. *Phys. Chem. Chem. Phys.* **2011**, *13*, 19663−19688.

(15) Caleman, C.; van Maaren, P. J.; Hong, M.; Hub, J. S.; Costa, L. T.; van der Spoel, D. Force Field Benchmark of Organic Liquids: Density, Enthalpy of Vaporization, Heat Capacities, Surface Tension, Isothermal Compressibility, Volumetric Expansion Coefficient, and Dielectric Constant. *J. Chem. Theory Comput.* **2012**, *8*, 61−74.

(16) Trokhymchuk, A.; Alejandre, J. Computer Simulations of Liquid/Vapor Interface in Lennard-Jones Fluids: Some questions and answers. *J. Chem. Phys.* **1999**, *111*, 8510−8523.

(17) Orea, P.; López-Lemus, J.; Alejandre, J. Oscillatory Surface Tension due to Finite-Size Effects. *J. Chem. Phys.* **2005**, *123*, 114702−114707.

(18) Zubillaga, R. A.; Labastida, A.; Cruz, B.; Martínez, J. C.; Sánchez, E.; Alejandre, J. Surface Tension of Organic Liquids Using the OPLS/AA Force Field. *J. Chem. Theory Comput.* **2013**, *9*, 1611−1615.

(19) Rowlinson, J. S.; Widom, B. *Molecular theory of capillarity*; Clarendon Press: 1982.

(20) Dang, L. X. Intermolecular interactions of liquid dichloromethane and equilibrium properties of liquid-vapor and liquid-liquid interfaces: A molecular dynamics study. *J. Chem. Phys.* **1999**, *110*, 10113−10122.

(21) Wang, L.-P.; Head-Gordon, T.; Ponder, J. W.; Ren, P.; Chodera, J. D.; Eastman, P. K.; Martinez, T. J.; Pande, V. S. Systematic Improvement of a Classical Molecular Model of Water. *J. Phys. Chem. B* **2013**, *117*, 9956−9972.

(22) Alejandre, J.; Chapela, G. A.; Saint-Martin, H.; Mendoza, N. A Non-Polarizable Model of Water that Yields the Dielectric Constant and the Density Anomalies of the Liquid: TIP4Q. *Phys. Chem. Chem. Phys.* **2011**, *13*, 19728−19740.

(23) Fuentes-Azcatl, R.; Alejandre, J. Non-Polarizable Force Field of Water Based on the Dielectric Constant: TIP4P/ϵ. *J. Phys. Chem. B* **2014**, *118*, 1263−1272.

(24) Fennell, C. J.; Libo, Li; Dill, K. A. Simple Liquid Models with Corrected Dielectric Constants. *J. Phys. Chem. B* **2012**, *116*, 6936−6944.

(25) Wang, L.-P.; Martinez, T. J.; Pande, V. S. Building Force Fields: An Automatic, Systematic, and Reproducible Approach. *J. Phys. Chem. Lett.* **2014**, *5*, 1885−1891.

(26) Horn, H. W.; Swope, W. C.; Pitera, J. W.; Madura, J. D.; Dick, T. J.; Hura, G. L.; Head-Gordon, T. Development of an Improved Four-Site Water Model for Biomolecular Simulations: TIP4P-Ew. *J. Chem. Phys.* **2004**, *120*, 9665−9678.

(27) Martin, M. G.; Siepmann, J. I. Transferable Potentials for Phase Equilibria. 1. United-Atom Description of n-Alkanes. *J. Phys. Chem. B* **1998**, *102*, 2569−2577.

(28) Chen, B.; Potoff, J. J.; Siepmann, J. I. Monte Carlo Calculations for Alcohols and Their Mixtures with Alkanes. Transferable Potentials for Phase Equilibria. 5. United-Atom Description of Primary, Secondary, and Tertiary Alcohols. *J. Phys. Chem. B* **2001**, *105*, 3093−3104.

(29) Wick, C. D.; Stubbs, J. M.; Rai, N.; Siepmann, J. I. Transferable Potentials for Phase Equilibria. 7. Primary, Secondary, and Tertiary Amines, Nitroalkanes and Nitrobenzene, Nitriles, Amides, Pyridine, and Pyrimidine. *J. Phys. Chem. B* **2005**, *109*, 18974−18982.

(30) Nath, S. K.; Escobedo, F. A.; de Pablo, J. J. On the simulation of vapor-liquid equilibria for alkanes. *J. Chem. Phys.* **1998**, *108*, 9905−9911.

(31) Nielsen, S. O.; Lopez, C. F.; Srinivas, G.; Klein, M. L. A coarse grain model for n-alkanes parameterized from surface tension data. *J. Chem. Phys.* **2003**, *119*, 7043−7049.

(32) Hess, B.; Kutzner, C.; van der Spoel, D.; Lindahl, E. GROMACS Algorithms for Highly Efficient, Load-Balanced, and Scalable Molecular Simulation. *J. Chem. Theory Comput.* **2008**, *4*, 435−447.

(33) Essmann, U.; Perera, L.; Berkowitz, M. L.; Darden, T.; Lee, H.; Pedersen, L. G. A smooth particle mesh Ewald method. *J. Chem. Phys.* **1995**, *103*, 8577−8593.

DOI: 10.1021/ct500853q
J. Chem. Theory Comput. 2015, 11, 683−693

(34) Merlet, C.; Salanne, M.; Rotenberg, B. New Coarse-Grained Models of Imidazolium Ionic Liquids for Bulk and Interfacial Molecular Simulations. *J. Phys. Chem. C* **2012**, *116*, 7687−7693.
(35) Shamsipur, M.; Beigi, A. A. M.; Teymouri, M.; Pourmortazavi, S. M.; Irandoust, M. Physical and electrochemical properties of ionic liquids 1-ethyl-3-methylimidazolium tetrafluoroborate, 1-butyl-3-methylimidazolium trifluoromethanesulfonate and 1-butyl-1-methylpyrrolidinium bis(trifluoromethylsulfonyl)imide. *J. Mol. Liq.* **2010**, *157*, 43−50.
(36) Noda, A.; Hayamizu, K.; Watanabe, M. Pulsed-Gradient Spin-Echo 1H and 19F NMR Ionic Diffusion Coefficient, Viscosity, and Ionic Conductivity of Non-Chloroaluminate Room-Temperature Ionic Liquids. *J. Phys. Chem. B* **2001**, *105*, 4603−4610.
(37) Wong, Ch.; Soriano, A.; Li, M. Diffusion coefficients and molar conductivities in aqueous solutions of 1-ethyl-3-methylimidazolium-based ionic liquids. *Fluid Phase Equilib.* **2008**, *271*, 43−52.
(38) Gregory, A. P.; Clarke, R. N. Traceable Measurements of the Static Permitivity of Dielectric Reference Liquids over the Temperature Range 5−50 °C. *Meas. Sci. Technol.* **2005**, *16*, 1506−1516.
(39) *CRC Handbook of Chemistry and Physics*, 88th ed.; Lide, D. R., Ed.; CRC: London, 2007.
(40) Smith, B. D.; Srivastava, R. *Thermodynamic data for pure compounds*; Elsevier: Amsterdam, 1986.
(41) Albright, P. S.; Gosting, L. J. Dielectric constants of the methanol-water system from 5 to 55 °C. *J. Am. Chem. Soc.* **1946**, *68*, 1061−1063.
(42) Chirico, R. D.; Steele, W. V.; Nguyen, A.; Klotsand, T. D.; Knipmeyer, S. E. Thermodynamic Properties of Pyridine-I. Vapor Pressure, High-temperature Heat Capacities, Densities, Critical Properties, Derived Thermodynamic Functions, Vibrational Assignment, and Derivation of Recommended Values. *J. Chem. Thermodyn.* **1996**, *28*, 797−818.
(43) Das, A.; Frenkel, M.; Gadallar, N. A. M.; Kudchadker, S.; Marsh, K. N.; Rodgers, A. S.; Wilhoit, R. C. Thermodynamic and Thermophysical Properties of Organic Nitrogen Compounds. Part II. 1- and 2-Butanamine, 2-Methyl-1-Propanamine, 2-Methyl-2-Propanamine, Pyrrole, 1-, 2-, and 3-Methylpyrrole, Pyridine, 2-, 3-, and 4-Methylpyridine, Pyrrolidine, Piperidine, Indole, Quinoline, Isoquinoline, Acridine, Carbazole, Phenanthridine, 1- and 2-Naphthalenamine, and 9-Methylcarbazole. *J. Phys. Chem. Ref. Data* **1993**, *22*, 659−782.
(44) Gonçalves, A. M. M.; Costa, C. S. M. F.; Bernardo, J. C. S.; Johnson, I.; Fonseca, I. M. A.; Ferreira, A. G. M. Dichloromethane: Revision and Extension of pρT Relationships for the Liquid. *J. Chem. Thermodyn.* **2011**, *43*, 105−116.
(45) García-Sánchez, F.; Romero-Martínez, A.; Trejo, A. Vapour Pressure, Critical Temperature, and Critical Pressure of Dichloromethane. *J. Chem. Thermodyn.* **1989**, *21*, 823−826.
(46) Liu, J.; Li, H.; Lin, J.-M. Measurements of Surface Tension of Organic Solvents Using a Simple Microfabricated Chip. *Anal. Chem.* **2007**, *79*, 371−377.

DOI: 10.1021/ct500853q
J. Chem. Theory Comput. 2015, 11, 683−693